

# Attaining Continuous Centimeter-Level Positioning on the Freeway in Combination with Error Detection

James W. Sinko and Joseph M. Strus, *SRI International*

## BIOGRAPHY

James W. Sinko is a Principal Engineer at SRI International. He received his B.S. (Engineering Science) and M.S.E.E. from Stanford University, and his Ph.D. (EE) from the University of Rochester. Dr. Sinko has been with SRI since 1967, working with radar and aircraft systems. For the last 9 years, he has been working with precision GPS for military and civil applications.

Joseph M. Strus is a Systems Analyst at SRI International where he has worked on precision navigation applications since 2001. Previously, he was a GPS Systems Engineer with the Government Systems Division of Rockwell Collins, Inc. Dr. Strus received his B.S. (1986) and Ph.D. (1994) in Mathematics from the University of Illinois at Urbana-Champaign.

## ABSTRACT

The development of reliable RTK GPS on most highways will enable many safety and convenience applications. An obvious application is vehicle lane departure warning. Eventually GPS could play an important role in fully automated highways. On the racetrack RTK GPS can show car handling characteristics and driver performance. Real-time centimeter-level accuracy GPS for highway and motor racing applications requires specialized algorithms. Some of the difficulties encountered on the freeway are the frequent obscurations that cause the receiver to lose track of the signal, severe multipath caused by nearby large trucks, and phase delays caused by trees and other obstacles alongside the roadway (phase delay measurements from trees are included). This causes a loss of the L2 carrier phase for several seconds and even after track is reestablished the accuracy is degraded for several seconds. A second difficulty in obtaining centimeter-level positioning using GPS is that the RTK solution occasionally is based on the wrong integers and gives a solution that may be off by up to several meters.

Our approach to the RTK GPS reliability problem has been to use two antennas and two GPS receivers on the vehicle along with an inertial measurement unit (IMU). A single

epoch RTK solution (relative to the base station) is generated for each of the receivers. Then the solutions are checked to see that the distance between the two antennas is close to the measured distance. Otherwise, both solutions can be rejected, and the calculated inertial position used. Under typical conditions, incorrect solutions on the freeway were reduced from 2.1 percent to 0.07 percent using this method with a single epoch RTK algorithm. This is because RTK solution errors are caused by local multipath and phase delays that do not affect each antenna in the same manner. Vehicular applications can use altitude aiding to help significantly in resolving the ambiguities. Code differential GPS and/or inertial calculations give the location on the road with sufficient accuracy that an accurate height can be found from a detailed road database and used as a constraint in finding the solution.

In addition to contributing to error detection, the IMU was used to maintain the continuity of the solution. To combine the RTK position and velocity with the inertial data, a 15 state extended Kalman filter is used. Since there are two antennas, azimuth initialization for the Kalman filter is from the two-dimensional GPS attitude system. Over a typical section of suburban freeway with overpasses and side obscurations, the combined system had a maximum horizontal error of 0.87 meter after a 29-second outage.

## INTRODUCTION

Low to moderate accuracy GPS automotive applications such as navigation, vehicle tracking, and stolen vehicle tracking are deployed in significant numbers today. Applications such as time-dependent toll collection and curve warning are starting to be deployed. Other applications that can be implemented with current code-based GPS technology include adaptive lighting, suspension, drive train control, and, with the addition of telematics-type communications, collision warning. Applications requiring knowledge of which lane a car is in can only marginally be done with code differential GPS. Navigation is enhanced by knowledge of which lane the vehicle is in because the driver can be advised to shift lanes for an upcoming turn or exit. Applications requiring lane knowledge include situation awareness displays (that show

all surrounding vehicles and their relative velocities, especially those in blind spots), and, for adaptive cruise control (ACC), determination of which lane the lead vehicle is in. However, the highest payoff GPS automotive applications require centimeter-level accuracy. These applications include lane departure warning and active lanekeeping (GPS/inertial measurement unit [IMU]-based steering). A more extensive discussion of highway applications appears in Venhovens et al. [1998].

Deployments of some of these advanced applications are already being attempted. However, these deployments are currently using camera-based technology, not GPS. Toyota is producing a minivan in Japan with a camera-based lane departure warning system. The Japanese Cima automobile (manufactured by Nissan) extends this idea even further with a system that “recognizes lane markings and feeds assistance to the steering to correct deviation from the traveling lane” [AEI, 2002]. The system is based on a camera that recognizes lane markers. Current research in fully automated automobiles is most active in Japan, and centers primarily on the use of magnetic nails and vision systems. RTK GPS is clearly accurate enough for these applications, and the applications will be more robust with the use of RTK GPS. In order to be competitive, the costs of both multifrequency GPS receivers and tactical grade IMUs will have to decrease dramatically.

Most RTK software and most dual frequency civilian receivers have been designed to operate in a relatively clear environment for surveying applications or for agricultural vehicles. Freeways require that RTK GPS work when large numbers of obstructions (overpasses, signs, other vehicles, hills, trees, and buildings) are present. A number of steps can be taken to improve the ability of RTK software to recover quickly from these obstructions. Some receivers perform better than others in this respect. Single-epoch ambiguity resolution algorithms are especially useful for rapidly recovering from obstructions. However, there is frequently doubt as to whether the new solution is correct. Map-derived altitude aiding (deriving height information

from a code-derived position and an accurate map of the road that gives height) has also proven useful.

## SINGLE-EPOCH FORMULATION

The single-epoch formulation is similar to that in Taniura et al. [1998] (see Eq. 1 that follows). The left side of the equation consists of the measured values minus the calculated values. The measured values include the double difference L1 phases, widelane phases, and pseudoranges. The unknown vector on the right-hand side of the equation will have the incremental changes (between each iteration) of the positions of the rover,  $x$ ,  $y$ ,  $z$ . If new satellites are used in the solution there will be changes in L1 integers ( $N_1, \dots, N_4$ ), and widelane integers ( $N_{w1}, \dots, N_{w4}$ ).

$L_{15}$  is the measured L1 double difference phase between satellite vehicles (SVs) 1 and 5, where 5 is the pivot SV,  $\rho_{15}$  is the computed double difference range,  $W_{15}$  is the measured double difference widelane phase, and  $P_{15}$  is the measured double-difference pseudorange. The last element of the left-hand vector and the last row of the design matrix are used only in the case of altitude aiding. Altitude aiding uses a differential code-based solution, and an accurate road map or database that contains accurate road heights to obtain height above the ellipsoid to within a few centimeters before attempting to find the RTK solution. To use altitude in aiding the solution, an extra measured minus calculated (height) is added in the list of measured minus calculated on the left-hand side of Eq. 1.  $H_m$  is the height found from the map, and  $H$  is the computed height. The difference between the rover and reference station is implied in all measured and calculated variables, but not explicitly shown. For simplicity, a minimum number of satellites (five in this case) is shown. For a more typical seven available SVs, thus six double differences, the left-hand vector will be  $19 \times 1$ , the design matrix will be  $19 \times 15$ , and the unknowns vector will be  $15 \times 1$ . If altitude aiding is not used, the corresponding dimensions would be  $18 \times 1$ ,  $18 \times 15$ , and  $15 \times 1$ .

$$\begin{bmatrix} L_{15} - \rho_{15} \\ L_{25} - \rho_{25} \\ L_{35} - \rho_{35} \\ L_{45} - \rho_{45} \\ W_{15} - \rho_{15} \\ W_{25} - \rho_{25} \\ W_{35} - \rho_{35} \\ W_{45} - \rho_{45} \\ P_{15} - \rho_{15} \\ P_{25} - \rho_{25} \\ P_{35} - \rho_{35} \\ P_{45} - \rho_{45} \\ H_m - H \end{bmatrix} = \begin{bmatrix} \partial \rho_{15} / \partial x & \partial \rho_{15} / \partial y & \partial \rho_{15} / \partial z & \lambda_1 & 0 & 0 & 0 & 0 & 0 & 0 & 0 & 0 \\ \partial \rho_{25} / \partial x & \partial \rho_{25} / \partial y & \partial \rho_{25} / \partial z & 0 & \lambda_1 & 0 & 0 & 0 & 0 & 0 & 0 & 0 \\ \partial \rho_{35} / \partial x & \partial \rho_{35} / \partial y & \partial \rho_{35} / \partial z & 0 & 0 & \lambda_1 & 0 & 0 & 0 & 0 & 0 & 0 \\ \partial \rho_{45} / \partial x & \partial \rho_{45} / \partial y & \partial \rho_{45} / \partial z & 0 & 0 & 0 & \lambda_1 & 0 & 0 & 0 & 0 & 0 \\ \partial \rho_{15} / \partial x & \partial \rho_{15} / \partial y & \partial \rho_{15} / \partial z & 0 & 0 & 0 & 0 & \lambda_w & 0 & 0 & 0 & 0 \\ \partial \rho_{25} / \partial x & \partial \rho_{25} / \partial y & \partial \rho_{25} / \partial z & 0 & 0 & 0 & 0 & 0 & \lambda_w & 0 & 0 & 0 \\ \partial \rho_{35} / \partial x & \partial \rho_{35} / \partial y & \partial \rho_{35} / \partial z & 0 & 0 & 0 & 0 & 0 & 0 & \lambda_w & 0 & 0 \\ \partial \rho_{45} / \partial x & \partial \rho_{45} / \partial y & \partial \rho_{45} / \partial z & 0 & 0 & 0 & 0 & 0 & 0 & 0 & \lambda_w & 0 \\ \partial \rho_{15} / \partial x & \partial \rho_{15} / \partial y & \partial \rho_{15} / \partial z & 0 & 0 & 0 & 0 & 0 & 0 & 0 & 0 & 0 \\ \partial \rho_{25} / \partial x & \partial \rho_{25} / \partial y & \partial \rho_{25} / \partial z & 0 & 0 & 0 & 0 & 0 & 0 & 0 & 0 & 0 \\ \partial \rho_{35} / \partial x & \partial \rho_{35} / \partial y & \partial \rho_{35} / \partial z & 0 & 0 & 0 & 0 & 0 & 0 & 0 & 0 & 0 \\ \partial \rho_{45} / \partial x & \partial \rho_{45} / \partial y & \partial \rho_{45} / \partial z & 0 & 0 & 0 & 0 & 0 & 0 & 0 & 0 & 0 \\ \partial H / \partial x & \partial H / \partial y & \partial H / \partial z & 0 & 0 & 0 & 0 & 0 & 0 & 0 & 0 & 0 \end{bmatrix} \times \begin{bmatrix} x \\ y \\ z \\ N_1 \\ N_2 \\ N_3 \\ N_4 \\ N_{w1} \\ N_{w2} \\ N_{w3} \\ N_{w4} \end{bmatrix} \quad (1)$$

The weighting matrix  $P$  allows the use of different standard deviations for each SV. It is formed from three separate submatrices, one for L1, one for widelane, and one for pseudorange. For the case of five satellites, each submatrix along the diagonal is  $4 \times 4$ , and there will be a single element along the diagonal for  $H$  so the weighting matrix is  $13 \times 13$ . Pseudoranges of low elevation satellites are heavily deweighted. More details on the weight matrix are given in Sinko [2001]. Integer ambiguities are resolved with the Lambda method [De Jonge and Tiberius, 1996].

### PHASE DISTORTION

To quantify some of the problems occurring in a highway environment, phase residuals of signals passing through trees were measured. L1/L2 measurement data were taken on a 250 meter baseline with one of the receivers set on a building near some pine trees so that occasionally one of the SVs would pass behind the trees. The other receiver was set in a location where there were no obstructions. Choke ring antennas were used for both receivers. The methodology was to look at the phase residuals of an SV that was not used in obtaining the RTK integers. This worked much better than just looking at the residuals when all SVs are used to obtain a solution because when a bad SV is used it tends to affect the residuals of all the other SVs. On all the tests, a second SV is taken out of the solution to show how the residuals of an unobscured SV appear.

Figure 1 shows the residuals of a satellite that passed through the edges of two pine trees (SV 26). SV 5 is included to give an idea of the residuals of an SV that was not obscured (a caution here is that the elevation angles of SV 5 do not closely match SV 26).  $C/N_0$  and elevation angles for SV 26 are also shown. For SV 26 there is some increase in the phase residuals, although part of the effect may be from the low elevation angle.

SV 8's path passed through the center of one of the pine trees (Figure 2). An appreciable drop in  $C/N_0$  occurred along with severe phase distortion (half a wavelength at times).  $C/N_0$  and elevation angles for SV 8 are also shown. The residuals of SV 7 are shown for comparison. Using SV 26's signal would cause severe problems in trying to resolve ambiguities.

SV 4's rising path passed through a poplar tree next to a building (see Figure 3). At the time the poplar tree had most of its leaves, although many of them had turned yellow. SV 2 is included to give an idea of the residuals of an SV that was not obscured.  $C/N_0$  and elevation angles for SV 4 are also shown. For SV 4 there is an appreciable increase in the phase residuals, but not as severe as for SV 26.

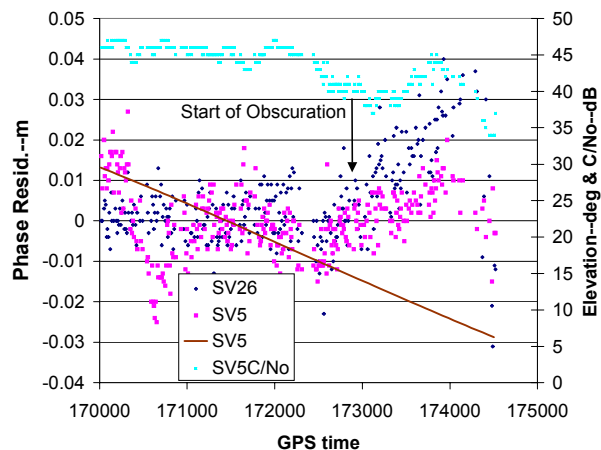


Figure 1: Phase residuals through pine tree foliage.

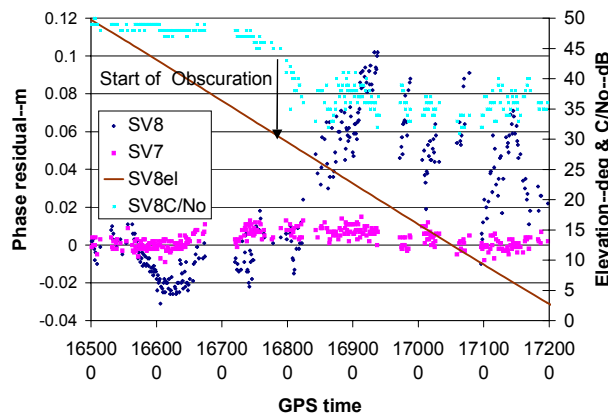


Figure 2: Phase residuals through the center of a pine tree.

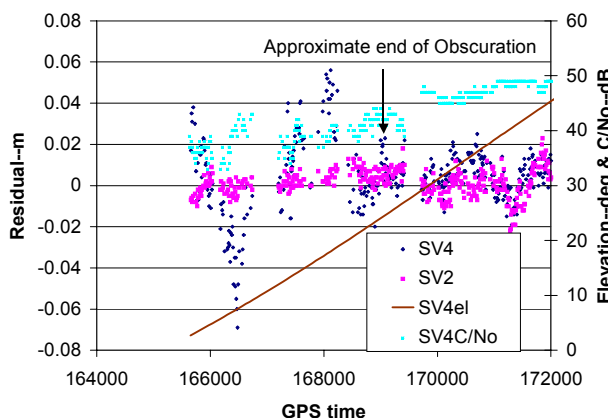


Figure 3: Phase residuals through the poplar tree foliage.

In summary, trees can cause serious carrier phase distortions that will cause problems for correct ambiguity resolution.

## ERROR CHECKING

In many situations this single epoch approach gives good results. In a typical freeway environment and under favorable satellite geometry it has given 92% correct solutions, and 8% unavailability (due to the receiver having five or fewer SVs in phase lock), even without using map aiding. However, under poor satellite geometry, and in areas where there are trees or other objects that cause phase distortion or code multipath, there can be significant numbers of errors.

One of the main problems with RTK GPS is knowing when one has the right answer. Low residuals and a low value of the ratio of the residuals of the best solution to the second best solution are two tests that can be made [Misra and Enge, 2001]. However, these tests discard many good solutions. Once one is confident of the solution, an additional check is to see that the integers do not change for the satellites that are common to both epochs.

On roads this method of error checking works quite well until an overpass is encountered. Then all satellites are lost and a method of verifying that a correct solution has been reestablished is needed. Since recovering phase lock and half cycle ambiguity can take 15 seconds or more, an IMU of the accuracy of the LN200 is marginal for checking the correctness of the GPS solution. The method we have adopted is to use two separate antennas and receivers and check to see if the distance between them measured by RTK GPS is consistent with the physical distance between them. Additionally, elevation angle is also checked to see that it is a reasonable value.

To conduct the tests, two antennas and receivers were mounted on a minivan (Figure 4): one antenna was mounted at the front center of the minivan roof, and one was located at the rear center of the roof and separated by a known distance. The RTK solution for each receiver was found, and then, based on these solutions, the distance between the two antennas was calculated. If the calculated differences varied significantly from the known distance, both solutions were rejected.

In addition to the GPS receivers a Litton LN200 IMU was mounted just below the rear antenna of the minivan. It was mounted on a heavy wood pylon bolted to the floor frame members to minimize any flexure effects. The roof of the minivan was not stiff enough to rigidly hold the IMU and its associated computer used to timestamp IMU data with GPS time. This location minimized any lever arm effects. Alternatively, using location information from the front antenna it was possible to test the Kalman filter's ability to handle a lever arm.

In addition to error checking, the two receivers were used as an attitude system. With the known baseline, the heading accuracy was estimated to have a standard

deviation of 0.2 degree. This is useful for quickly seeding the Kalman filter with a reasonably accurate heading.

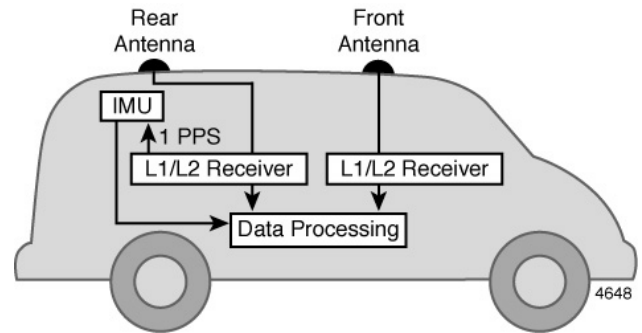


Figure 4: Configuration of minivan.

## KALMAN FILTER

The extended Kalman filter was chosen as the method of sensor integration. Because of the continuous high-rate nature of the INS data, the Navigation processor output is used to provide a reference trajectory. The filter then processes errors in the system as well as estimating INS sensor errors.

There are two generic GPS/INS integration schemes generally considered today: one based on feeding the GPS position to the filter (which we will call solution based, but which is sometimes called loosely coupled), and the other that feeds individual satellite measurements to the filter (which we will call measurement based, but which is sometimes called tightly coupled<sup>1</sup>). In the solution-based mode, the GPS and INS are treated as separate navigation processes, and generally, the GPS position and/or velocity is used as an input to the filter. The GPS position/velocity output is typically derived either by a separate Kalman filter or by a least squares type algorithm. In the measurement-based mode, the GPS pseudorange or carrier phase and raw INS measurements are inputs into the filter. A discussion of the relative merits of the two types of filters appears in Farrell and Barth [1999] and Schertzing [2000].

For our application, the solution-based filter was chosen largely because of the simplicity and independence from the GPS processing task. Time constraints warranted a comparatively quick integration solution as well as the fact that several other applications were to be considered. When there are fewer than four satellites, the measurement-based system can still make use of the limited measurements that are available. However, its advantages may be limited in freeway overpass situations because phase lock is typically lost on all satellites. Overpasses

<sup>1</sup> Other authors reserve the term tightly coupled to systems in which the IMU measurements are used to control tracking loops in the GPS receiver.

generally account for the longest outages experienced in a freeway environment.

Our filter has 15 states. The error modeling used for the state transition matrix is similar to ones that appear in more detail in Farrell et al. [1998] and Ford et al. [2001]. The measurement inputs are the RTK positions.

### ROADWAY TESTS

The vehicle path of the San Carlos US101 freeway experiment is shown in Figure 5. The epochs with GPS solutions are denoted by a broad red line. The narrow blue line is where the receiver had phase lock on four or fewer SVs after encountering an overpass or other obstruction. The small area near the center with many turns is an airport parking area with few obstructions where a number of turns were made to initialize the Kalman filter. The main GPS outages are numbered to correspond to data in Figure 6. The freeway path begins and ends in the middle of the right side. At the north end, the vehicle passes beneath an overpass, and proceeds up a cloverleaf with many trees, which causes an extended outage. After crossing over the freeway, the vehicle again passes beneath an overpass. Another overpass is encountered southbound. The south portion of the path exits the freeway, passes over the freeway and encounters another overpass when entering the freeway. The missing data points are all because of recovery time from overpasses or trees encountered. These data were taken at a 2 Hz rate, although some runs were taken at 10 Hz.

RTK data in Figure 5 were among the worst of experiments we have run on this section of freeway with only 81% of epochs on the freeway having a correct solution on both the front and back receivers. For some unknown reason the vast majority of incorrect solutions came from the back receiver. This data set was chosen because it illustrates the performance of the IMU and Kalman filter when they are not receiving GPS measurements. The horizontal errors are illustrated in Figure 6. The largest error was 0.87 meter for a 29-second outage at an exit overpass followed by extensive tree coverage on the cloverleaf that leads to crossing over the freeway at the north end of the route. To see if the altitude changes and 270 degree turn associated with the cloverleaf were part of the problem, a simulated 34-second outage was introduced on the southeast cloverleaf. The resulting error was only 0.54 meter. Figure 7 shows the run with 30-second simulated outages occurring every 130 seconds. The RMS horizontal error of the real and simulated outages is 0.84 meter and the average outage was 28 seconds. Figure 8 shows the difference between the two antenna derived RTK heading and the Kalman filter heading. The variance is compatible with our estimate of 0.2 degree for the RTK measurements. The bias is probably a result of the IMU not being perfectly aligned with the two antennas.

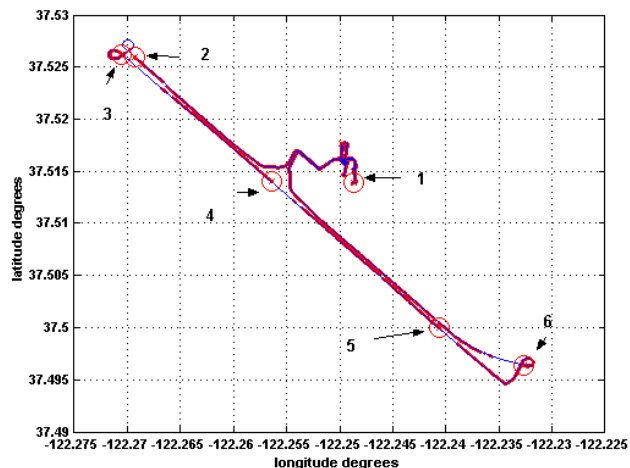


Figure 5: Highway test area (on left) and airport parking area. Actual outages are numbered.

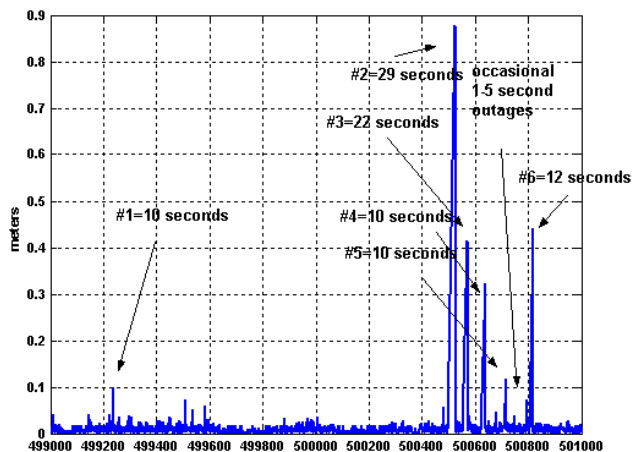


Figure 6: Horizontal position error after real GPS outages.

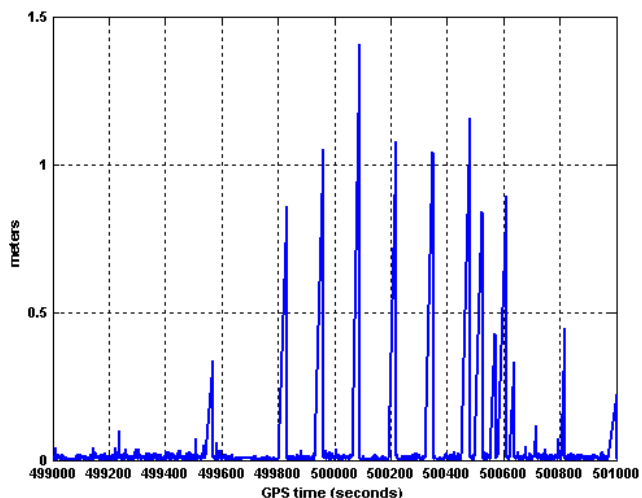
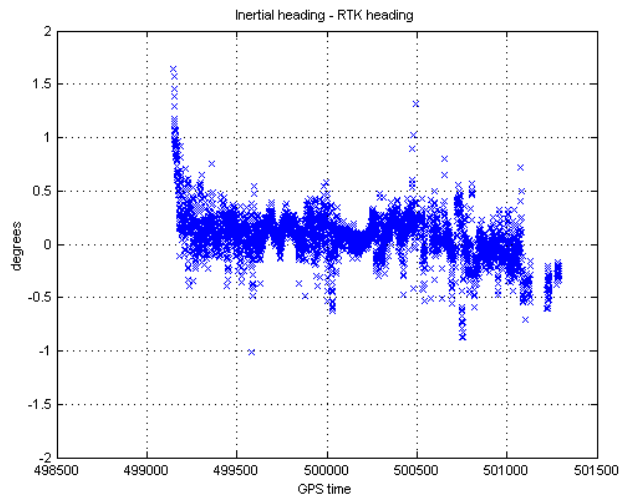


Figure 7: Horizontal position error after simulated GPS outages.



**Figure 8:** Difference between inertial and RTK heading.

### AIRCRAFT TESTS

In order to test the Kalman filter under more dynamic conditions, tests were conducted in a Cessna 182 aircraft. The GPS receiver and IMU were located in the mostly up facing rear window of the aircraft. The GPS antenna had some blockage because of the metal around the window. Single epoch RTK performed well when the aircraft was heading north, but not as well when heading south. Hence, a version of the program that held integers constant during portions of the flight was used. The test consisted of three standard rectangular landing pattern flights. During the first pattern, only 30 degree turns were made at the corners of the pattern. During the second pattern, several 30 degree Dutch rolls were performed. During the third pattern, several 30 degree pitch changes were performed. Figure 9 shows the landing pattern and denotes where the simulated outages occurred. Figure 10 shows the difference between the output of the Kalman filter with simulated 30-second outages and the RTK GPS solution. The RMS average of the outage errors is 0.64 meter. Overall, the filter seems to perform at least as well in the air as in a vehicle, even though the speeds were substantially greater and the IMU was of slightly lower quality. Part of the reason may be that the steeper pitch and roll maneuvers allowed better determination of the roll and pitch gyro biases.

### OUTLOOK

Vehicular applications of RTK will have to overcome the problems of signal blockage, integrity, and cost. C/A code on L2 will help the recovery time after encountering obstacles. L5 will increase the availability and reliability of integer ambiguity resolution, and, when combined with inertial systems, may provide a reasonable measure of integrity. The realization of the Galileo system would provide more satellites, which is helpful for overcoming obscurations. Many obstacle situations will require that

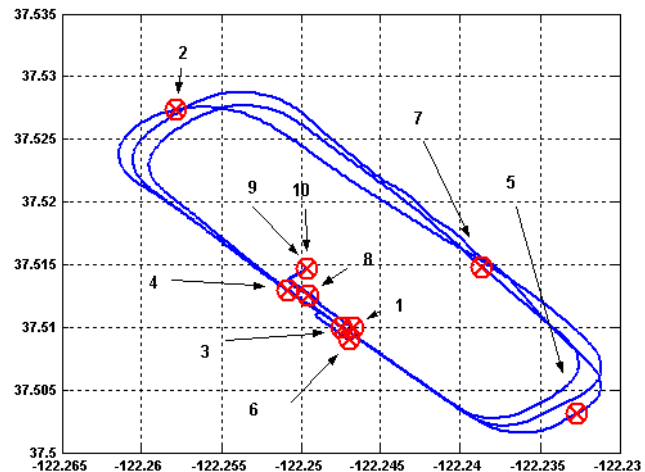


**Figure 9:** Airport landing pattern and positions of simulated outages.

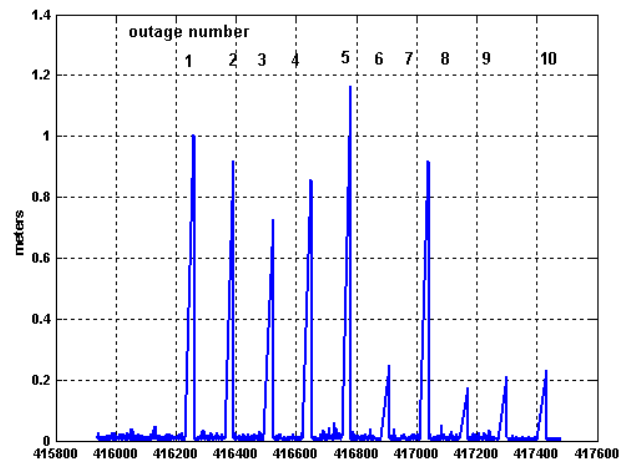


**Figure 10:** Aircraft horizontal position error after simulated GPS outages.

inertial and/or wheel sensor measurements be incorporated into the system. Additional sensors such as vision systems and magnetic nails could be used in conjunction with RTK GPS. These additional sensors can also aid in establishing integrity. Pseudolites can enhance the reliability of ambiguity resolution, enhance integrity, and extend the use of RTK GPS into obscured locations.

RTK GPS will need to be aided by other sensors in areas where the satellites are obscured. The most promising sensors are inertial. The coupling of the inertial system's short-term relative accuracy with RTK GPS's ability to give absolute location is very attractive. Systems such as magnetic nails and vision systems (both demonstrated at the Automated Highway Demonstration 1997 in San Diego) can be viewed as either alternatives to GPS or as adjuncts to GPS. Presently, it does not appear that any of these systems can offer the versatility and reliability to be

the sole system in safety critical applications (such as vehicle steering or automated highways). Rather, a combination of some of these systems will be required to attain the availability and integrity.

It is interesting to note that automated farming is an active area of development in the US and may be a predecessor to the development of automated highway vehicles.

The practicality of RTK GPS for automotive control applications is critically dependent on the availability of low-cost receivers and IMUs. Presently, low cost receivers appear feasible, but the case for low cost IMUs with adequate accuracy is less certain.

## CONCLUSIONS

The system described herein can reliably locate a vehicle on a typical freeway to within a few centimeters when GPS is available. Techniques such as integer following can ensure the validity of integer ambiguity resolution when continuous tracking is maintained. However, the problem of establishing the validity of the integer solution after all satellites are lost is best solved by having two separate antennas and receivers with a known baseline.

GPS outages are inevitable in the freeway environment, and the IMU provides good accuracy for outages of a few seconds. When the GPS outage is as long as 30 seconds the accuracy degrades to about 0.5 meter RMS while using a tactical grade IMU.

## ACKNOWLEDGMENTS

Ford Motor Company generously loaned us a Litton LN200, allowing us to begin this work several months before the arrival of the unit we ordered.

## REFERENCES

- AEI [2002] Chassis Trends, Automotive Engineering International, August 2002, pp 31–33, SAE International.
- De Jonge, P., and C. Tiberius [1996] The LAMBDA Method for Integer Ambiguity Estimation: Implementation Aspects. LGR-Series No. 12, Publications of the Delft Computing Centre.
- Farrell, J.A., M. Barth, R. Galijan, and J. Sinko [1998] GPS/INS Lateral and Longitudinal Control Demonstration, Final Report, California Partners for Advanced Transit and Highways.
- Farrell, J.A., and M. Barth [1999] The Global Positioning System and Inertial Navigation, McGraw-Hill.
- Ford, T., J. Neumann, P. Fenton, M. Bobye, and J. Hamilton [2001] OEM4 Inertial: A Tightly Integrated Decentralized Inertial/GPS Navigation System, ION-GPS 2001.
- Misra, P., and Enge, P. [2001] Global Positioning System Signals, Measurements, and Performance, Ganga-Jamuna Press.
- Taniura, K., K. Fuse, and S. Takahashi [1998] “Instantaneous Dual Frequency Ambiguity Resolution,” Institute of Navigation, ION-NTM-98, pp. 781–790, Long Beach, California.
- Schertzinger, B.M. [2000] Precise Robust Positioning with Inertial/GPS RTK, ION-GPS 2000.
- Sinko, J.W. [2001] Single-Epoch Ambiguity Resolution for Highway and Racetrack Applications, ION-GPS 2001.
- Venhovens, P., J. Bernasch, J. Lowenau, H. Rieker, and M. Schraut [1998] The Application of Advanced Vehicle Navigation in BMW Driver Assistance Systems. 99PC-240 (Society of Automotive Engineers, Inc.).